Measurement of the Hadronic Photon Structure Function $F_2^\gamma(x, Q^2)$ at ALEPH

Johannes Heß
Siegen University
ALEPH Collaboration
PHOTON 2003, Frascati, April 7th., 2003

- ★ Motivation
- ★ Experiment
- ★ Data Selektion
- ★ Unfolding - Problem and Method
- ★ Background and Selection
- ★ Results
- ★ Systematic Uncertainties
- ★ Conclusions

Two-Photon Interaction

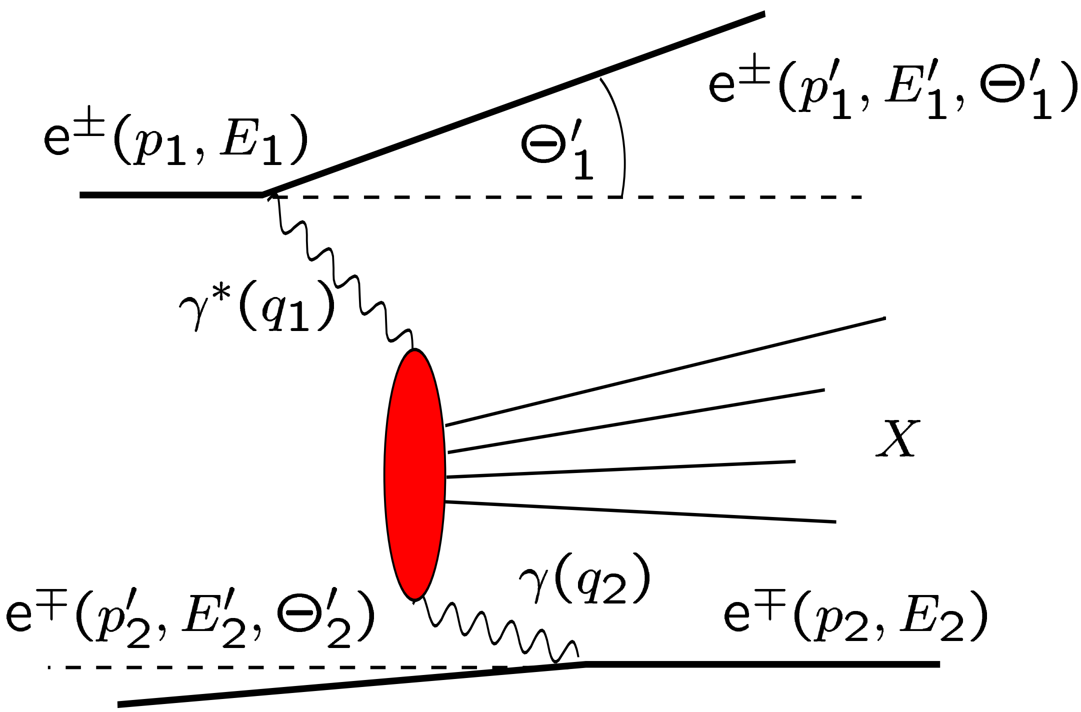

Commonly used variables and Lorentz invariants

$$
\begin{aligned}
Q^2 &= -q_1^2 = (p_1 - p_1')^2 \approx 2EE_1'(1 - \cos\Theta_1') \\
P^2 &= -q_2^2 = (p_2 - p_2')^2 \approx 2EE_2'(1 - \cos\Theta_2') \\
x &= \frac{Q^2}{2q_2 \cdot q_1} = \frac{Q^2}{W^2 + Q^2 + P^2} \\
y &= \frac{q_2 \cdot q_1}{p_1 \cdot q_2} \\
z &= E_\gamma / E \\
W^2 &= (q_1 + q_2)^2 \approx 4E_{\gamma_1}E_{\gamma_2}
\end{aligned}
$$

Cross Section

$$
\begin{aligned}
d\sigma &= d\sigma(e^+e^- \to e^+e^-\gamma^*\gamma^* \to e^+e^- X) \\
&= \frac{\alpha_{em}^2}{16\pi^4 q_1^2 q_2^2}\left[\frac{(q_1q_2)^2 - q_1^2 q_2^2}{(p_1p_2)^2 - m_e^2 m_e^2}\right]^{\frac{1}{2}} \\
& \quad [4\rho_1^{++}\rho_2^{++}\sigma_{TT} + 2\rho_1^{++}\rho_2^{00}\sigma_{TL} + \\
& \quad 2\rho_1^{00}\rho_2^{++}\sigma_{LT} + \rho_1^{00}\rho_2^{00}\sigma_{LL} - \\
& \quad 2|\rho_1^{+-}\rho_2^{+-}|\tau_{TT}\cos 2\tilde{\phi} + \\
& \quad 8|\rho_1^{+0}\rho_2^{+0}|\tau_{TL}\cos\tilde{\phi}]\frac{d^3p_1' d^3p_2'}{E_1' E_2'}
\end{aligned}
$$

with

σ_{xx}	:	Cross section $\gamma^*\gamma^* \to X$ for polarized photons (T: transversal, L: longitudinal)
τ_{xx}	:	Interference terms
$\tilde{\phi}$	:	Angle between lepton scattering planes in $\gamma\gamma$-cm system
ρ^{ab}	:	Helicity-density matrix, $a, b = +, -, 0$

Contribution of eγ-vertices can be separated (Equivalent Photon Approximation).
$\Rightarrow$ can be calculated in QED

Single Tag

The cross section simplifies for single tag events:

Tag: scattered leptons are detected
$\rightarrow$ Four momentum of the photon is known

Scattering angle is usually small and leptons escape through the beam pipe.

Single Tag
$\rightarrow$ Four momentum transfer on the undetected lepton is small

Cross section can be approximated for

$$P^2 \approx 0,$$

Measurement integrates over $\tilde{\phi}$.

Definition of Structure Functions

$$
\begin{aligned}
2xF_T^\gamma(x,Q^2) &= \frac{Q^2}{4\pi^2\alpha}\sigma_{TT}(x,Q^2) \\
F_2^\gamma(x,Q^2) &= \frac{Q^2}{4\pi^2\alpha}\left[\sigma_{TT}(x,Q^2)+\sigma_{LT}(x,Q^2)\right] \\
F_L^\gamma(x,Q^2) &= \frac{Q^2}{4\pi^2\alpha}\sigma_{LT}(x,Q^2)
\end{aligned}
$$

Differential cross section:

$$
\begin{aligned}
\frac{\mathrm{d}^4\sigma}{\mathrm{d}x\mathrm{d}Q^2\mathrm{d}z\mathrm{d}P^2} &= \frac{\mathrm{d}^2N_\gamma^T}{\mathrm{d}z\mathrm{d}P^2}\frac{2\pi\alpha^2}{xQ^2} \\
&\quad \left[(1+(1-y)^2)F_2^\gamma(x,Q^2)\right. \\
&\quad \left.-y^2F_L^\gamma(x,Q^2)\right].
\end{aligned}
$$

Current of incoming transversally polarized quasi-real photos (from EPA):

$$
\frac{\mathrm{d}^2N_\gamma^T}{\mathrm{d}z\mathrm{d}P^2} = \frac{\alpha}{2\pi}\left[\frac{1+(1-z)^2}{z}\frac{1}{P^2}-\frac{2m_e^2z}{P^4}\right]
$$

$$
F_2^\gamma(x,Q^2) \sim \frac{\mathrm{d}^2\sigma}{\mathrm{d}x\mathrm{d}Q^2}
$$

for $y^2 \ll 1$

ALEPH

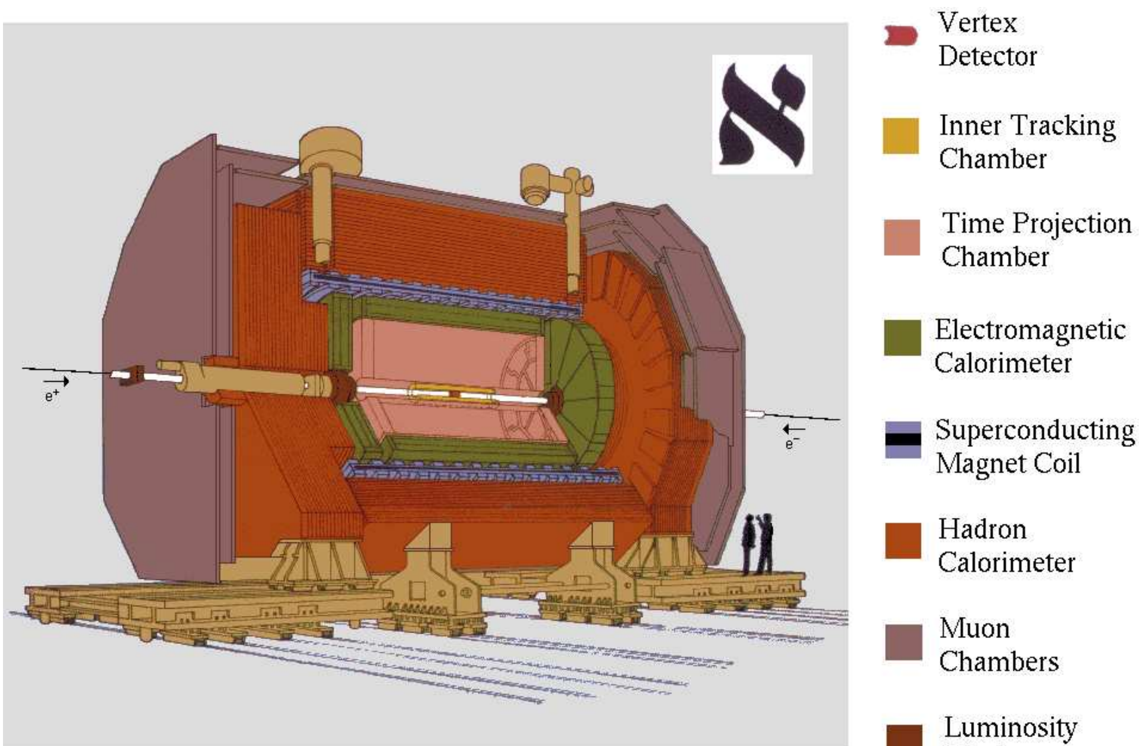

The ALEPH Detector

SiCAL

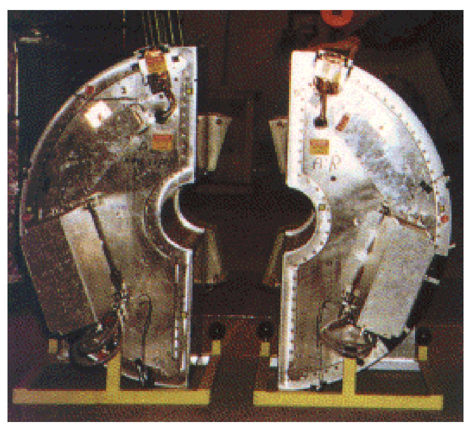

LCAL

Typical Event

... Single Tag in SiCAL:

Made on 5-Mar-2002 16:12:28 by hess with DALI_E2.
Filename: DC050075_015121_020305_1612.PS

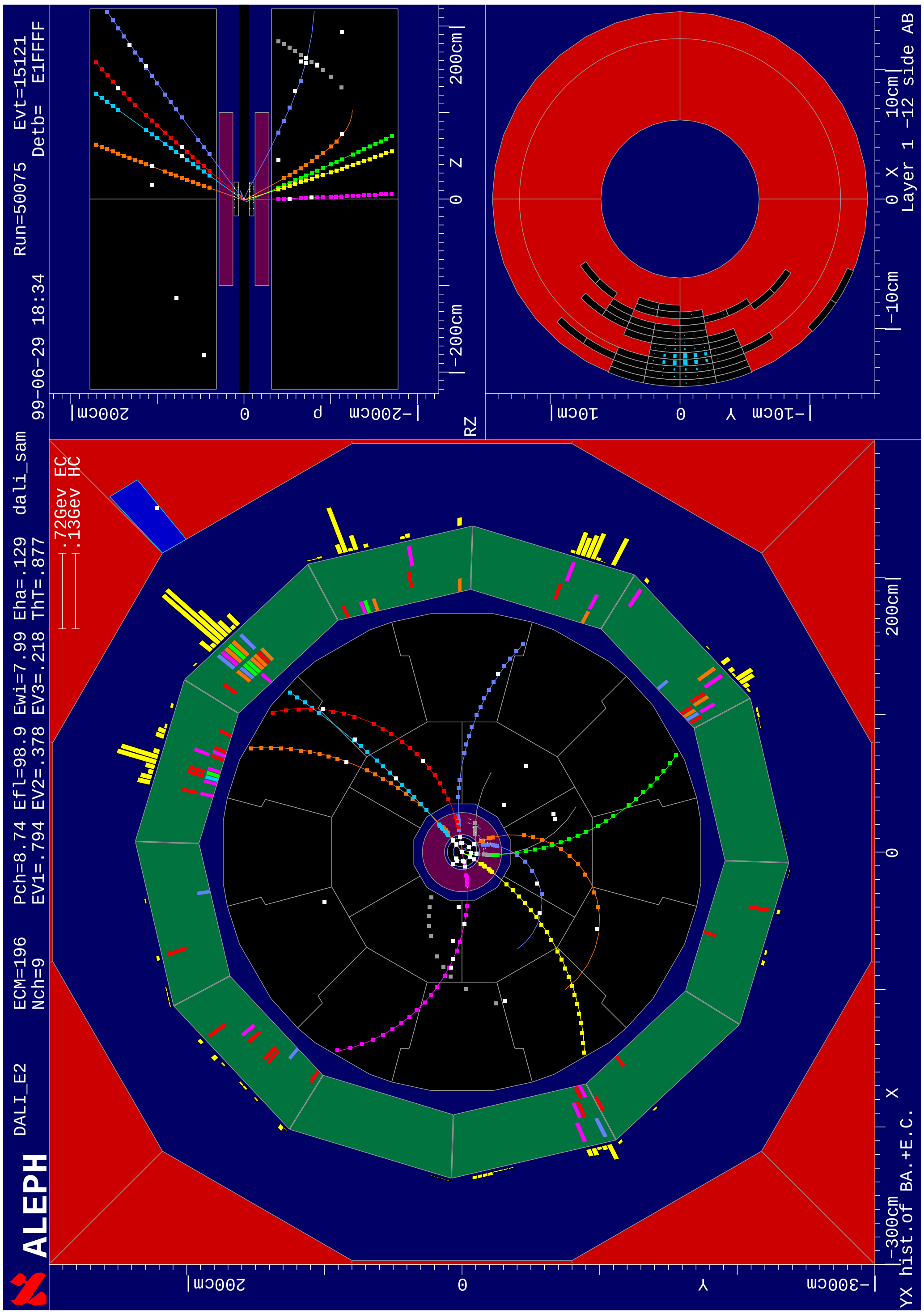

Typical Event

... Single Tag in LCAL:

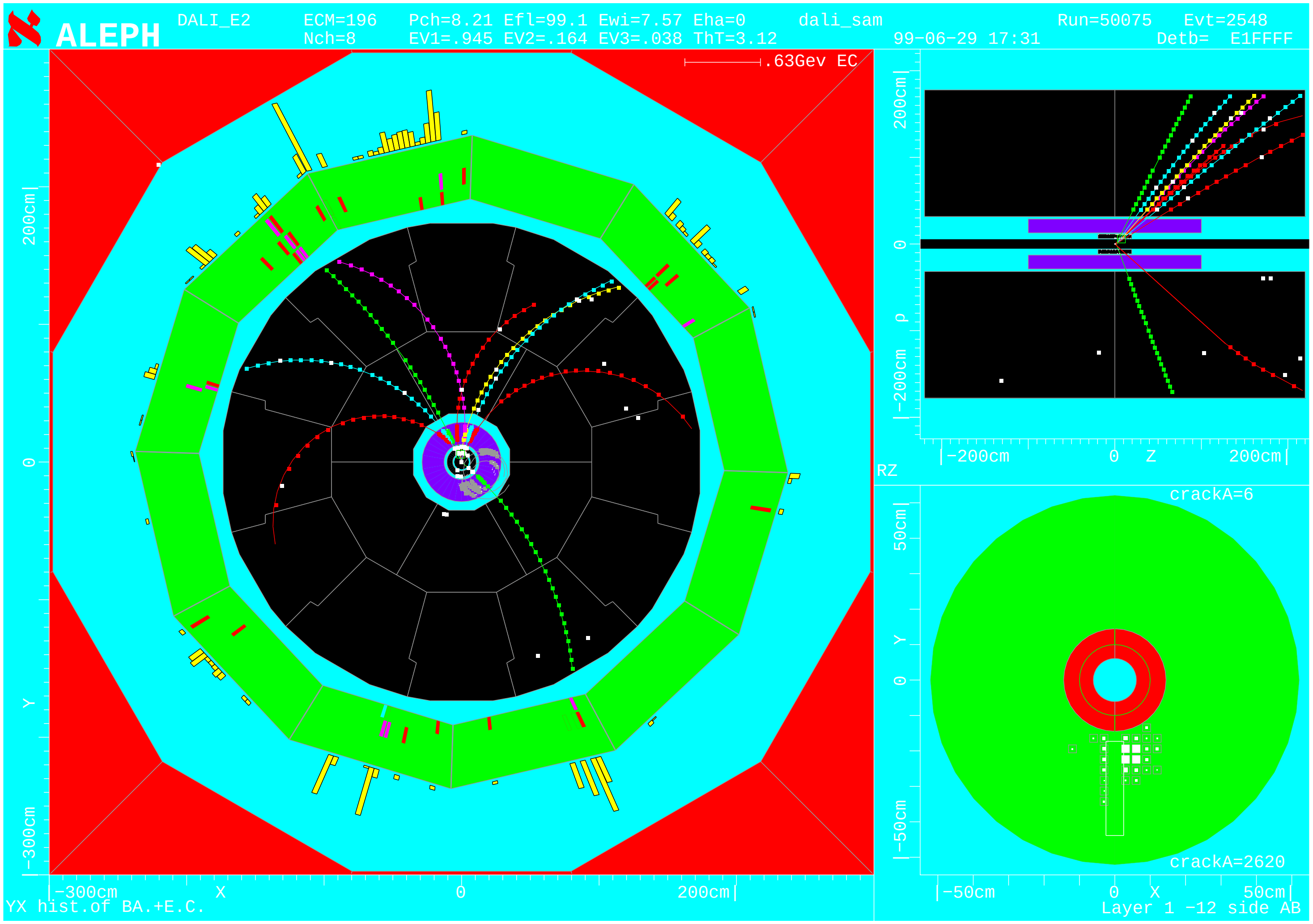

Made on 5-Mar-2002 16:22:11 by hess with DALI_E2.
Filename: DC050075_002548_020305_1622.PS

Background I

dominant Background:

Off-Momentum Electrons

can be treated by special cuts:
(Details Gerrit Prange)

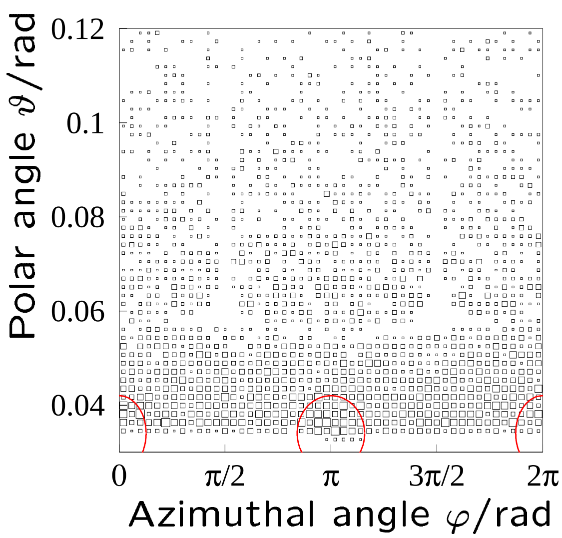

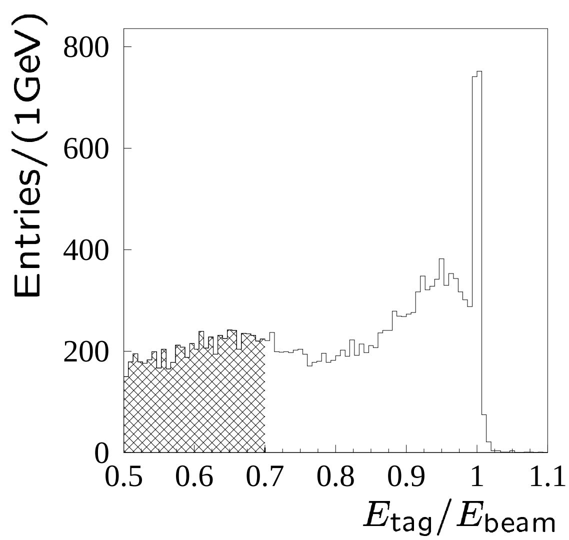

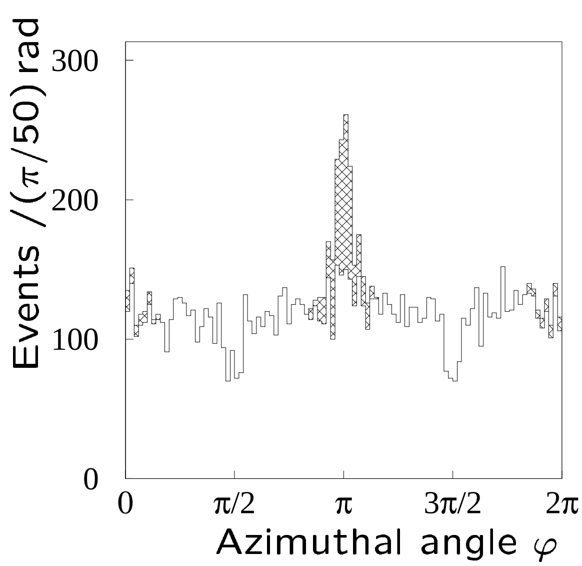

⇐ φ-Spectrum
after all
selection cuts

Background II

Process	Contamination [%]			
	$\langle Q^2 \rangle = 17.3\text{GeV}^2$			
	189GeV	196GeV	200GeV	$205-207$GeV
$\gamma\gamma \to e^+e^-$	0.22±0.03	0.26±0.05	0.25±0.05	0.27±0.09
$\gamma\gamma \to \mu^+\mu^-$	< 0.1			
$\gamma\gamma \to \tau^+\tau^-$	3.4±0.1	3.9±0.1	4.1±0.1	4.3±0.1
$e^+e^- \to q\bar{q}$	0.24±0.01	0.23±0.01	0.24±0.01	0.22±0.01
$e^+e^- \to \mu^+\mu^-$	< 0.1			
$e^+e^- \to \tau^+\tau^-$	< 0.1			
$e^+e^- \to We\nu$	< 0.1			
$e^+e^- \to Zee$	0.15±0.01	0.14±0.01	0.16±0.01	0.15±0.01
Q^2 migration	4.97±0.06	4.17±0.05	3.80±0.05	2.50±0.04
	$\langle Q^2 \rangle = 67.2\text{GeV}^2$			
	189GeV	196GeV	200GeV	$205-207$GeV
$\gamma\gamma \to e^+e^-$	0.3±0.04	0.22±0.05	0.31±0.07	0.41±0.14
$\gamma\gamma \to \mu^+\mu^-$	< 0.1			
$\gamma\gamma \to \tau^+\tau^-$	6.1±0.2	6.6±0.2	7.1±0.2	7.0±0.2
$e^+e^- \to q\bar{q}$	0.88±0.02	0.91±0.02	0.93±0.02	0.98±0.03
$e^+e^- \to \mu^+\mu^-$	< 0.1			
$e^+e^- \to \tau^+\tau^-$	< 0.1			
$e^+e^- \to We\nu$	< 0.1			
$e^+e^- \to Zee$	0.61±0.01	0.55±0.02	0.58±0.02	0.62±0.02
Q^2 migration	1.72±0.04	1.63±0.04	1.79±0.04	2.35±0.05

Contamination of the selected data sample through background processes.

Background III

Migration effects occur especially for the low Q^2 region.

They cannot be treated by the response matrix but have to be subtracted like background.

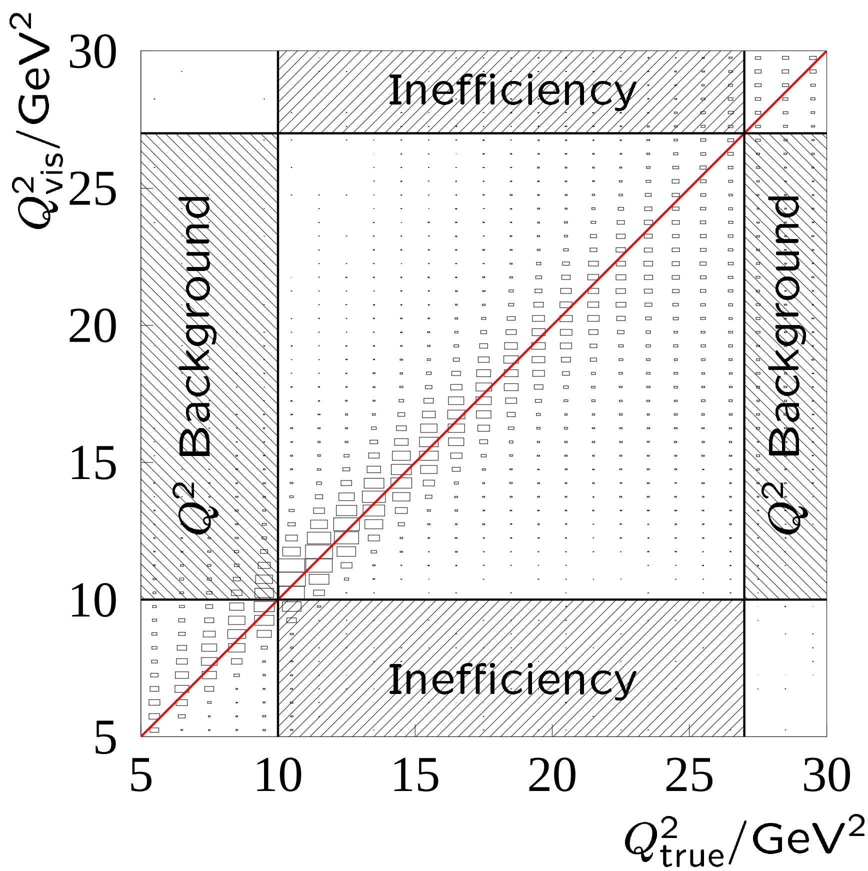

Final Selection Cuts

Due to different background and acceptance conditions
different cm-Energies are treated separately.

Almost all cuts are identical:

$$
\begin{aligned}
E_{\text{Tag}} &\geq 70\% \times E_{\text{Beam}} \\
W_{\text{had}} &\geq 3.5\,\text{GeV für unteren } Q^2 \text{ Bereich} \\
&\geq 3\,\text{GeV für oberen } Q^2 \text{ Bereich} \\
E_{\text{vis}} &\leq 70\,\text{GeV} \\
N_{e^\pm} &= 0 \\
N_{\mu^\pm} &= 0
\end{aligned}
$$

Energy-Flow objects are used!

Off-Momentum-Cuts

$$
\begin{aligned}
E_{\text{Tag}} &> 0.7 \cdot E_{\text{beam}} \\
\text{.AND.} & \\
\Big[\text{If } E_{\text{Tag}} &< 0.8 \cdot E_{\text{beam}} \\
\text{then} & \\
1 &< \left(\frac{\varphi-\pi}{HA_\varphi}\right)^2 + \left(\frac{\frac{\pi}{2}-\left|\frac{\pi}{2}-\vartheta\right|-0.035}{HA_\vartheta}\right)^2 \text{ .AND.} \\
1 &< \left(\frac{\pi-|\pi-\varphi|}{HA_\varphi}\right)^2 + \left(\frac{\frac{\pi}{2}-\left|\frac{\pi}{2}-\vartheta\right|-0.035}{HA_\vartheta}\right)^2\Big] .
\end{aligned}
$$

$$
\begin{aligned}
HA_\vartheta &= 8\,\text{mrad, and} \\
HA_\varphi &= 5\,\text{mrad} .
\end{aligned}
$$

Selected Events

E_{cms} /GeV	Luminosity /pb^{-1}	Number of events	Q^2 range /GeV^2	$\langle Q^2\rangle$ /GeV^2
189	177.0	5411 3537	10-27 27-250	16.1 61.7
196	82.6	2577 1643	10-28 28-250	16.7 65.7
200	87.8	2694 1648	10-29 29-250	17.4 68.3
205-207	201.0	6167 3560	10-32 32-250	18.4 72.9
$\sum$	548.4	16849 10388	$\langle Q^2\rangle = 17.3\text{GeV}^2$ $\langle Q^2\rangle = 67.2\text{GeV}^2$	

Number of selected events after all cuts listed for all centre-of-mass energies and Q^2 ranges. The range of Q^2 of the two bins analyzed is given in column three. The mean value of the virtualities $\langle Q^2\rangle$ is calculated and listed in the fourth column. No background has been subtracted at this stage.

Comparison with Monte Carlo

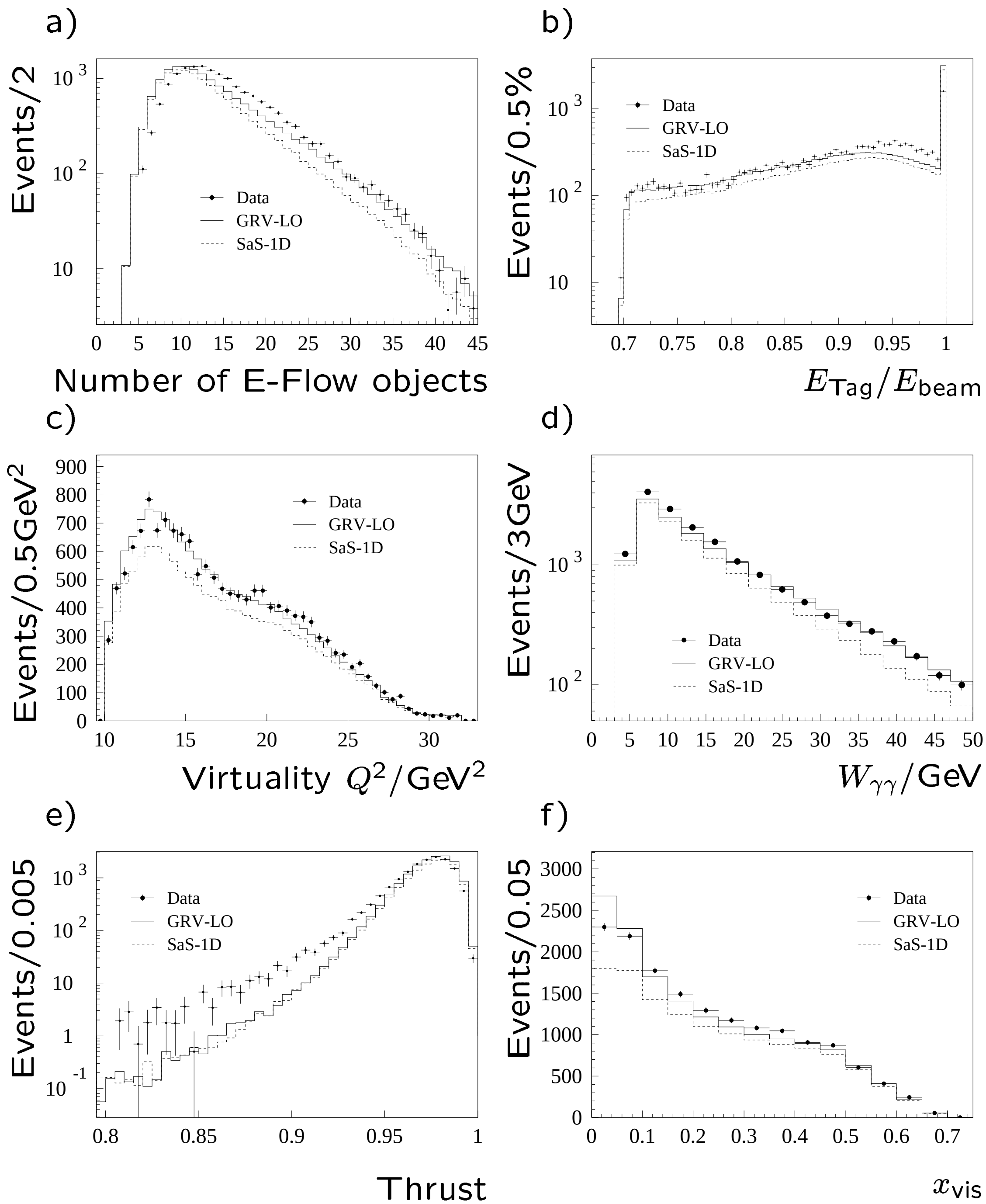

Comparison of data and Monte Carlo simulations for the sample with $\langle Q^2 \rangle = 17.3\mathrm{GeV}^2$. The histograms are HERWIG simulations using a GRV-LO parameterization (solid line) and a SaS-1D set of parameters (dashed line) for the input structure function. ALEPH data with backgrounds subtracted are shown with full errors. All histograms are normalized to the data luminosity.

Comparison with Monte Carlo

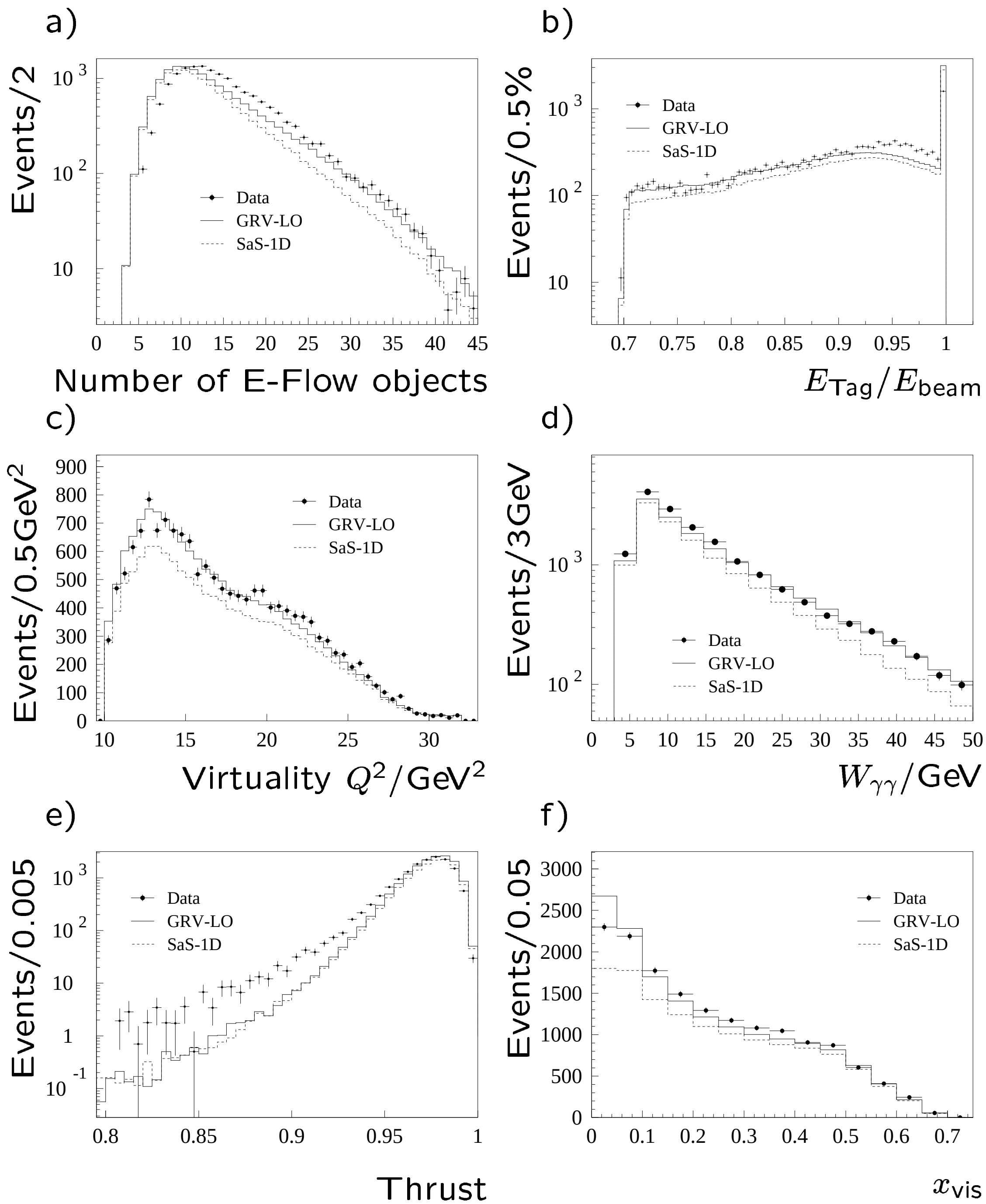

Same plots as in Fig. , but for the high Q^2 region with $\langle Q^2 \rangle = 67.2\text{GeV}^2$.

Fragmentation

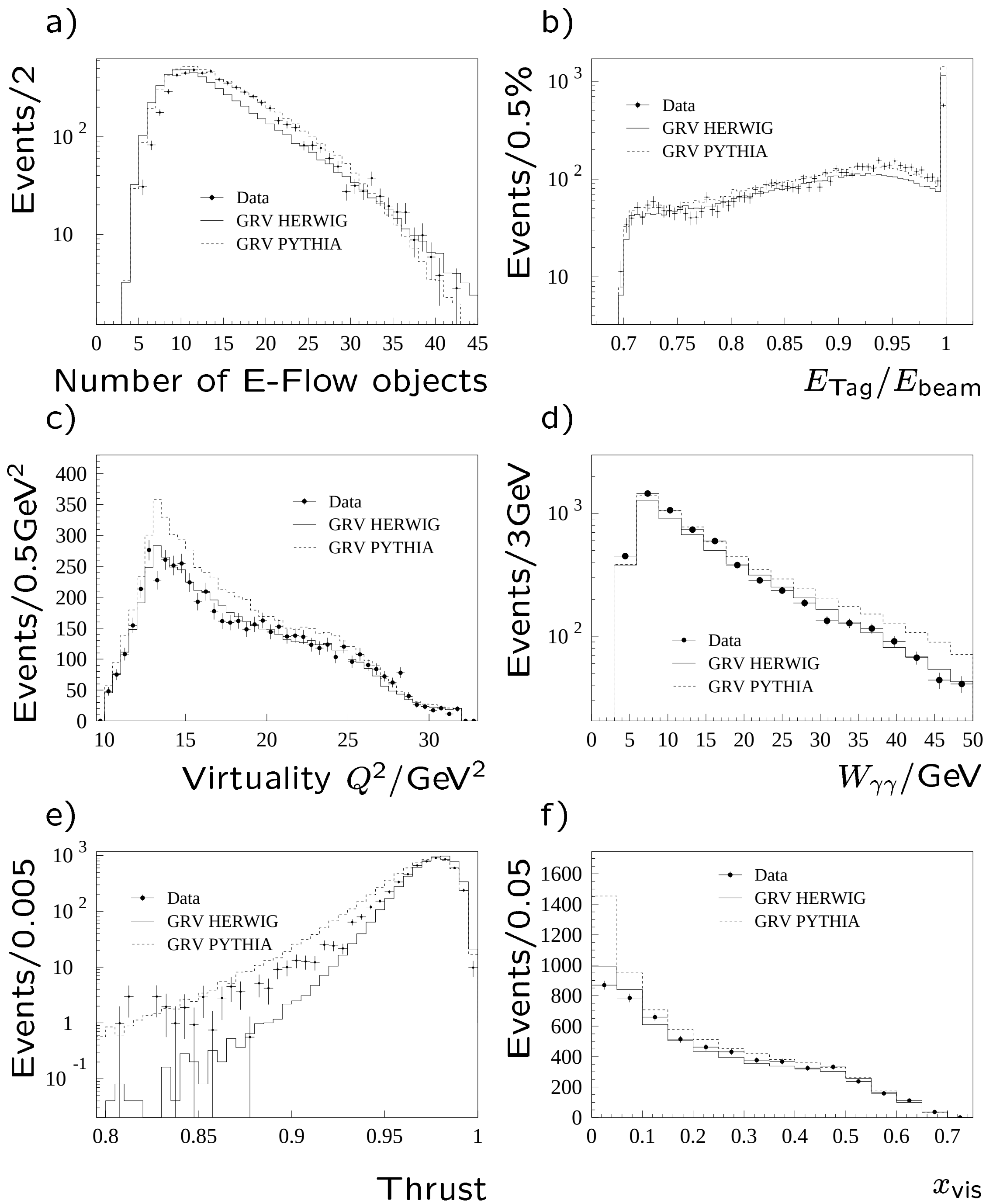

The same quantities are shown as in Fig. , but in this case the data are compared to Monte-Carlo simulations from the two different generators HERWIG (solid line) and PYTHIA (dashed line). In both cases the GRV-LO parameterization is used. $\langle Q^2 \rangle = 17.3\mathrm{GeV}^2$.

Fragmentation

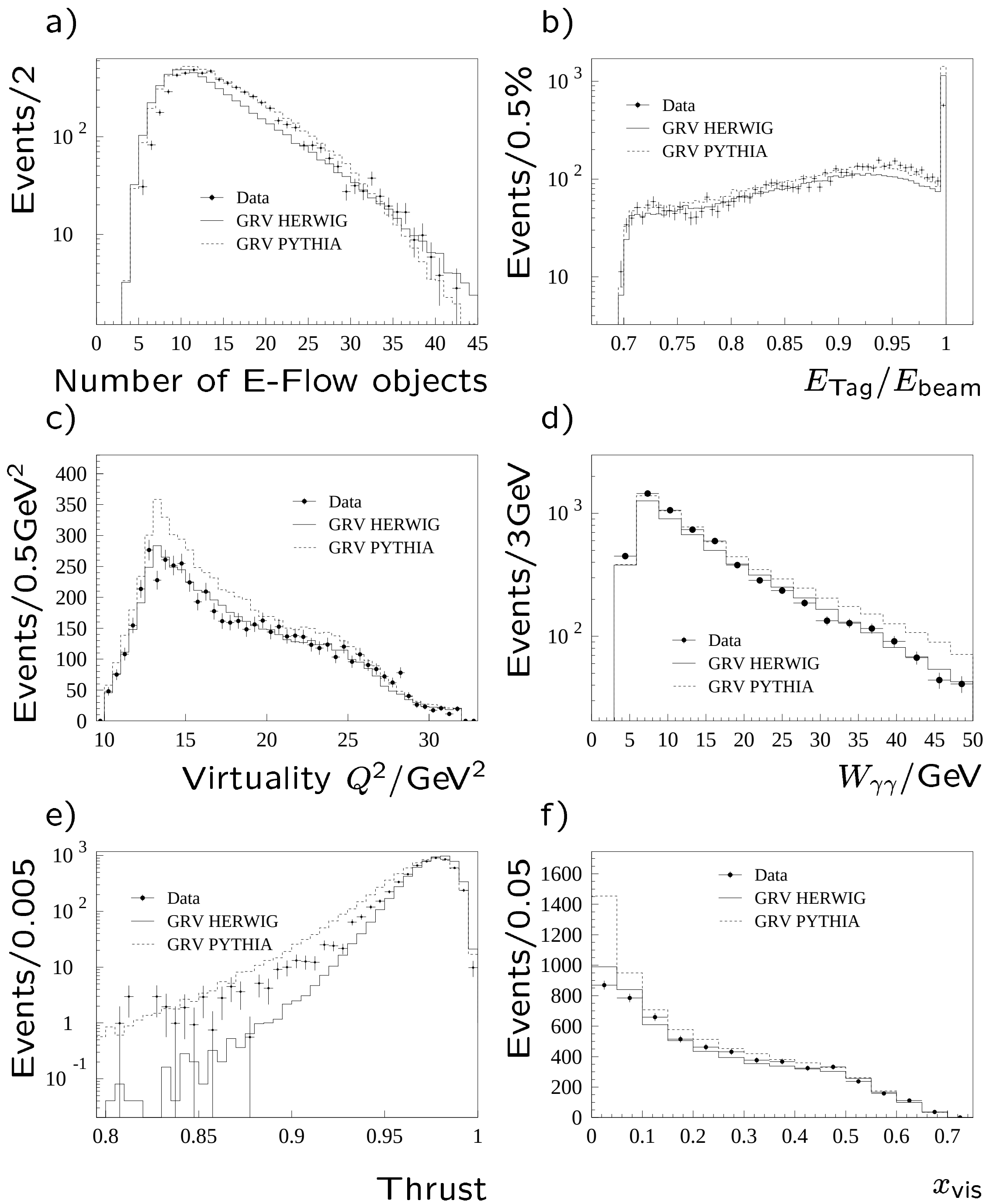

Same plots as in Fig. but for the high Q^2 region with $\langle Q^2 \rangle = 67.2\text{GeV}^2$.

Detector Acceptance

LEP is excellent for $\gamma\gamma$-Physics,
BUT
ALEPH was not designed for that.

Problems arise from strong Lorentz-boost of the $\gamma\gamma$-events:
Large part of the hadr. system leave the detector undetected.

$\Rightarrow$ Measurement of x is poor!

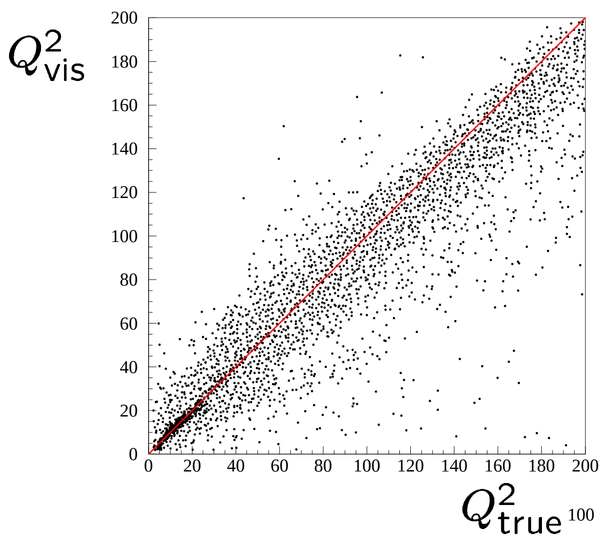

Q^2-Measurement is relatively good,

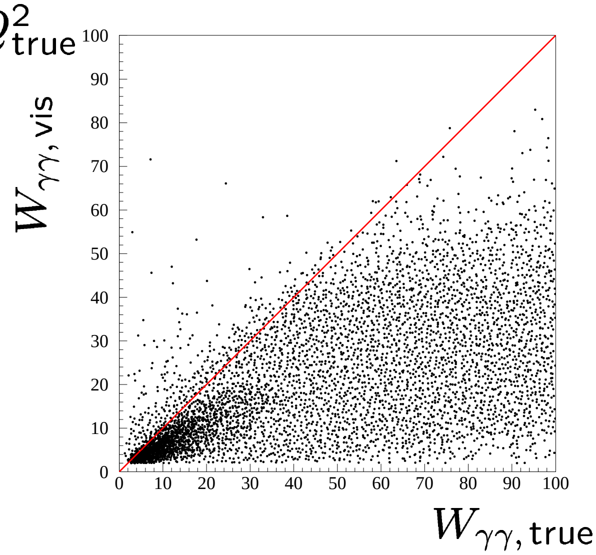

the $W_{\gamma\gamma}$-Measurement is not!

Resolution

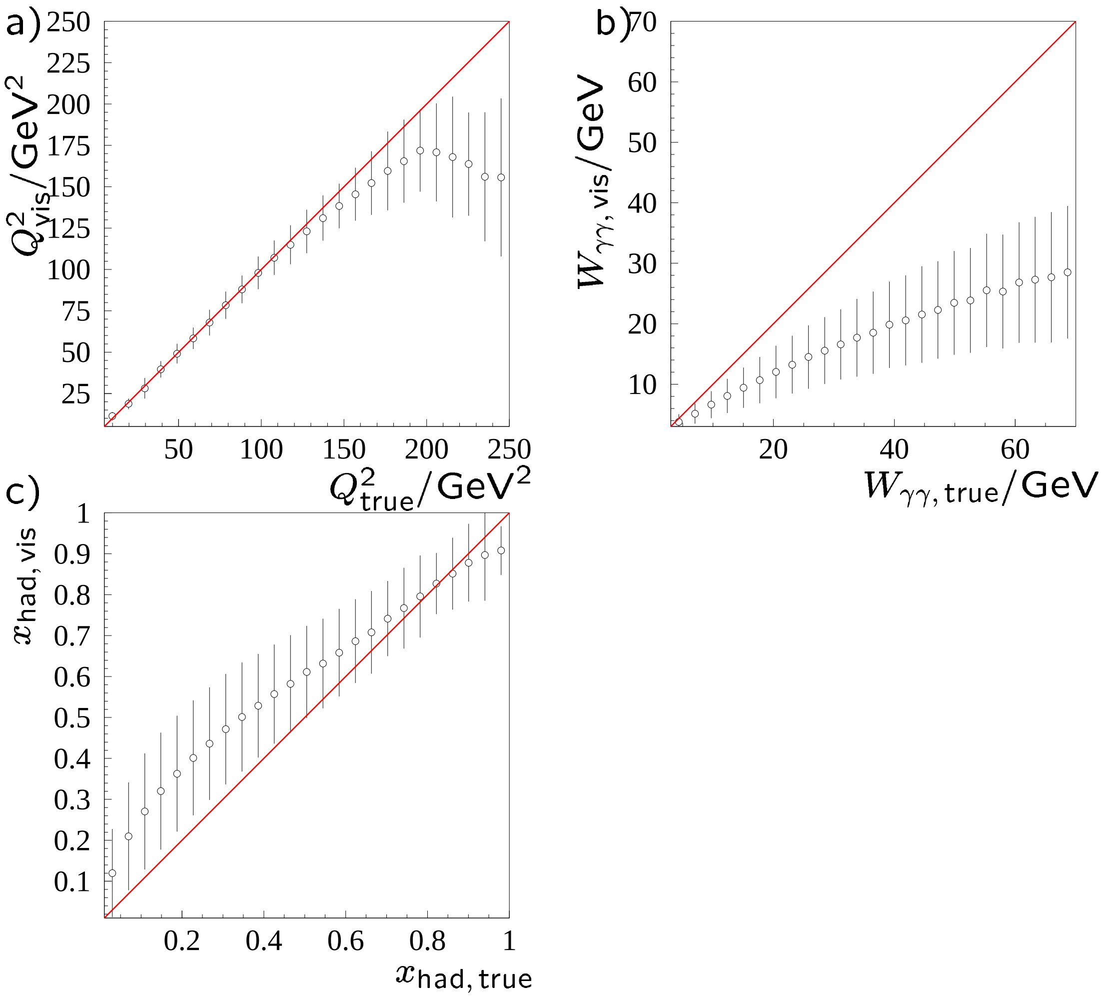

Resolution of a) the virtuality Q^2 of the probing photon, b) the invariant hadronic mass in the final state and c) the Bjorken variable x. The reconstructed quantity is plotted versus the true values from Monte-Carlo simulations. The mean observed value and the standard deviation is plotted for events generated in a certain bin in the truth distribution. While the resolution of Q^2 is limited by the energy measurement in the luminosity calorimeter, the discrepancy between observed and generated $W_{\gamma\gamma}$ is mainly caused by undetected final state particles.

Detector Response Matrix

wanted	:	$d\sigma/dx$ from x_{true}-Spectrum
seen	:	x^{δ}_{vis}

The effect of the detector can be expressed by a Matrix:

$$A\mathbf{x}_{\text{true}} = \mathbf{x}^{\delta}_{\text{vis}}$$

A can be obtained from from MC-calc. with full detector simulation.

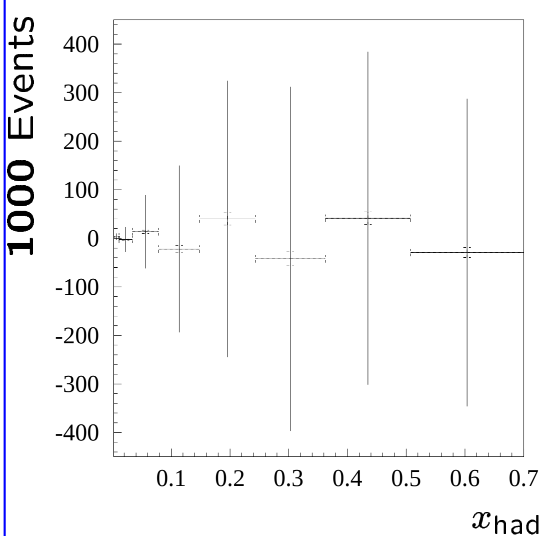

unregularized x_{unfolded}

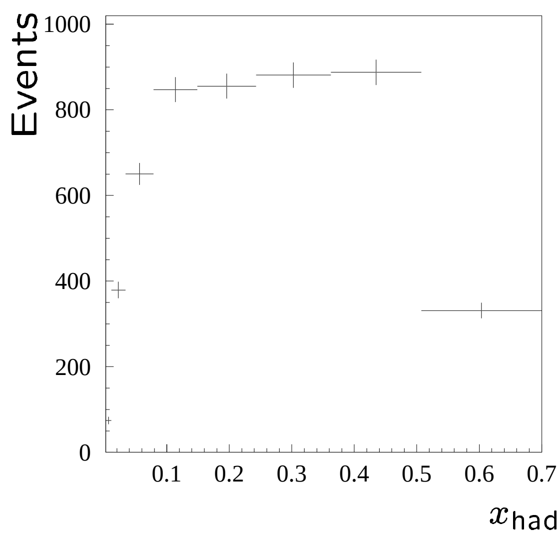

x_{vis}

Ill-conditioned Systems

Small fluctuations in the measured distribution y^δ lead to large uncertainties in x_{unfold}:

$$\frac{||\Delta x||}{||x||} \leq \text{cond}(A) \frac{||\Delta y||}{||y||}$$

Condition of the Matrix A:

$$\text{cond}(A) := ||A|| \, ||A^{-1}||$$

for Hermitian Matrix A and Euklidian norm:

$$\text{cond}(A) = \frac{|\lambda_{\text{max}}|}{|\lambda_{\text{min}}|}$$

with Eigenvalues λ.

Uncertainties of the matrix have to be taken into account as well:

$$\frac{||x^\delta - x||}{||x||} \leq \frac{\text{cond}(A)}{1 - ||A^{-1}|| \, ||A^\delta - A||} \left\{ \frac{||y^\delta - y||}{||A|| \, ||x||} + \frac{||A^\delta - A||}{||A||} \right\}$$

Way out:

The Condition of the systems has to be improved!

Tikhonov Regularization

Contribution of different singular values are weighted with

$$\frac{\mu_i^2}{\alpha + \mu_i^2}.$$

α: Regularization parameter, $\alpha \geq 0$

$$x_\alpha = \sum_{j=1}^{r} \frac{\mu_j}{\alpha + \mu_j^2}(y, v_j)u_j$$

is unique solution of the equation

$$(\alpha I + A^\top A)x_\alpha = A^\top y.$$

For a measurement y^δ with

$$||y^\delta - y||_2 \leq \delta < ||y^\delta||_2, \quad \delta > 0$$

there is a unique $\alpha = \alpha(\delta) > 0$, so that x_α solves

$$||Ax_\alpha - y^\delta||_2 = \delta,$$

It is

$$x_\alpha \to A^\dagger y \quad \text{für} \quad \delta \to 0$$

$\alpha(\delta)$ can be calculated explicitly.

Backfoldtest

How does the “regularized spectrum“ agree with the measured data?

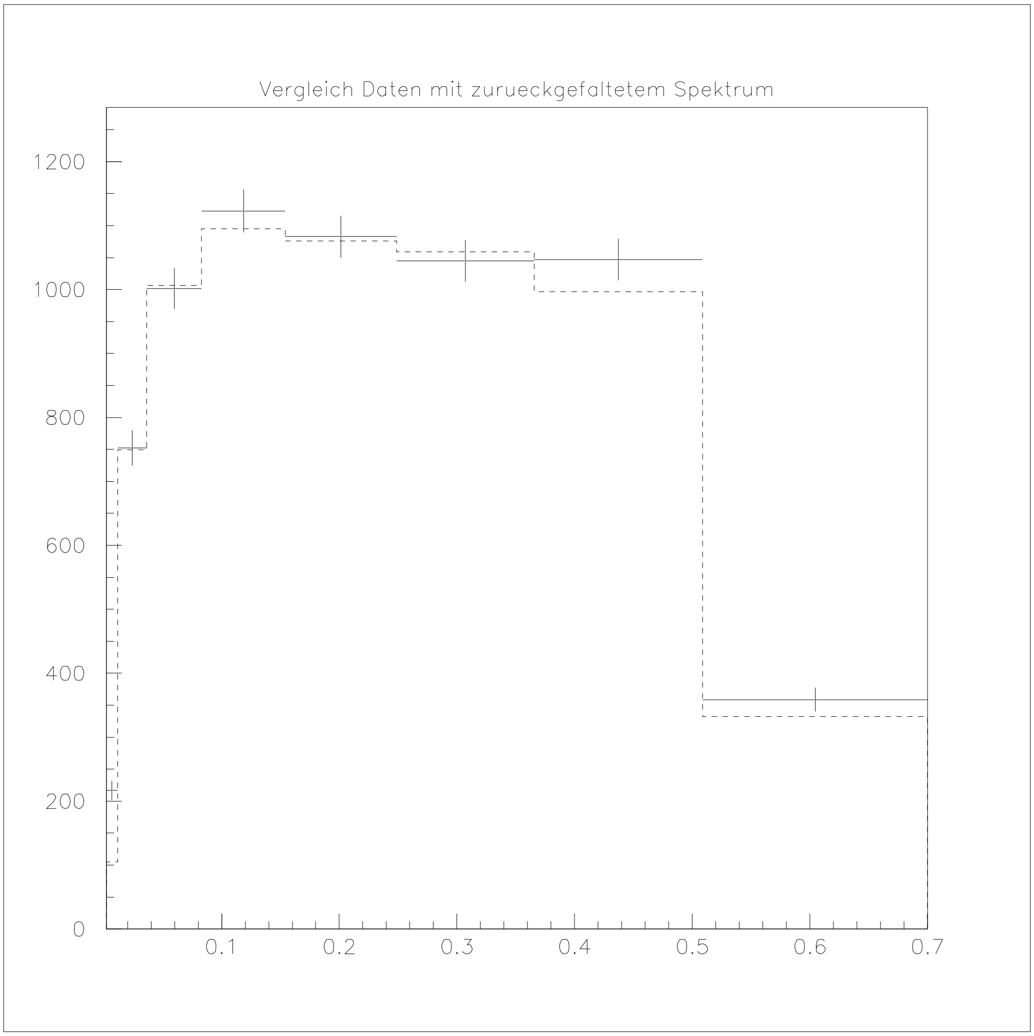

dashed: back folded spectrum after regularization

Uncertainties

What does a pretty distribution cost?

$$\begin{aligned} x_\alpha - x &= (\alpha I + A^\top A)^{-1} A^\top (y^\delta - y) + \\ &\quad (\alpha I + A^\top A)^{-1} A^\top y - A^\dagger y \end{aligned}$$

and

$$\begin{aligned} ||x_\alpha - x||_2 &\leq ||(\alpha I + A^\top A)^{-1} A^\top||_2 \delta + \\ &\quad ||(\alpha I + A^\top A)^{-1} A^\top y - A^\dagger y||_2 \end{aligned}$$

as an estimate for

$$E_{\text{total}} \leq E_{\text{data}} + E_{\delta \text{A}} + E_{\text{approx}}.$$

$E_{\text{data}} + E_{\delta\text{A}}$: calculated from error propagation

E_{approx}: not accessible from data, can be estimated from theor. Models (Monte-Carlo).

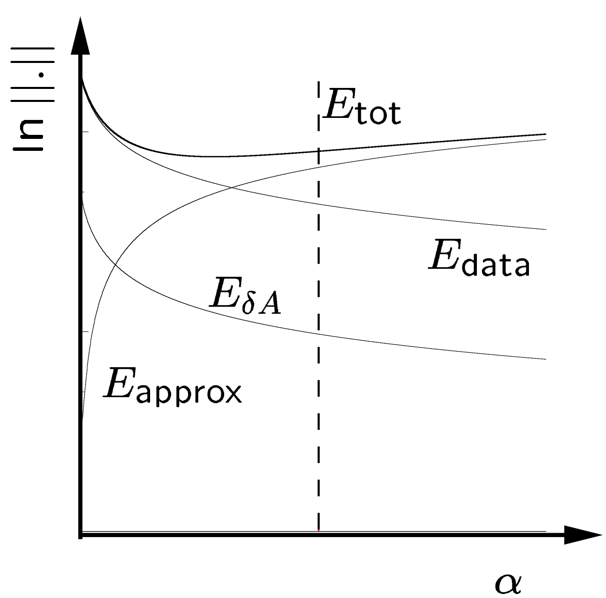

Uncertainties II

Sources of Uncertainties

- Statistical errors
- Systematic uncertainties
  - Approximation error from regularization
  - Model dependence of the detector matrix
  - Fragmentation
  - Limited Monte-Carlo statistics
  - Energy resolution/calibration
  - Momentum resolution/calibration
  - Treatment of P^2
  - Selection cuts
  - Trigger efficiency

Statistical Uncertainties

Covarianzmatrix

Without regularization:

$$C_x = A_0^{-1} C_y A_0^{-1\,\top} + $$
$$+ A_0^{-1} \left(\delta_{ij} \sum_k \left[\left(\bar{\mathbf{x}}_k^2 + \left(\sigma_k^{(1)} \right)^2 \right) \sigma^2(A_{ik}) \right] \right) A_0^{-1\,\top}$$

With regularization ($R = A^{-1\,\top} \left(\alpha I + A^\top A \right)$):

$$\begin{aligned} C_{x,\alpha} = \; & R_0^{-1} C_y R_0^{-1\,\top} + \\ & + R_0^{-1} \left(\delta_{ij} \sum_k \left(R_0^{-1} \left(\bar{\mathbf{y}} \bar{\mathbf{y}}^\top + C_y \right) R_0^{-1\,\top} \right)_{kk} \sigma^2(A_{ik}) \right) R_0^{-1\,\top} + \\ & + R_0^{-1} A_0^{-1\,\top} \left(\delta_{ij} \sum_k \left(A_0 R_0^{-1} - \mathbf{1} \right) \left(\bar{\mathbf{y}} \bar{\mathbf{y}}^\top + C_y \right) \left(R_0^{-1\,\top} A_0^\top - \mathbf{1} \right) \sigma^2(A_{ki}) \right) A_0^{-1} R_0^{-1\,\top} + \\ & + R_0^{-1} \left(\left[R_0^{-1} \left(\bar{\mathbf{y}} \bar{\mathbf{y}}^\top + C_y \right) \left(R_0^{-1\,\top} A_0^\top - \mathbf{1} \right) \right]_{ji} \sigma^2(A_{ij}) \right) A_0^{-1} R_0^{-1\,\top} + \\ & + R_0^{-1} A_0^{-1\,\top} \left(\left[\left(A_0 R_0^{-1} - \mathbf{1} \right) \left(\bar{\mathbf{y}} \bar{\mathbf{y}}^\top + C_y \right) R_0^{-1\,\top} \right]_{ji} \sigma^2(A_{ji}) \right) R_0^{-1\,\top} \end{aligned}$$

Differential Cross Sections

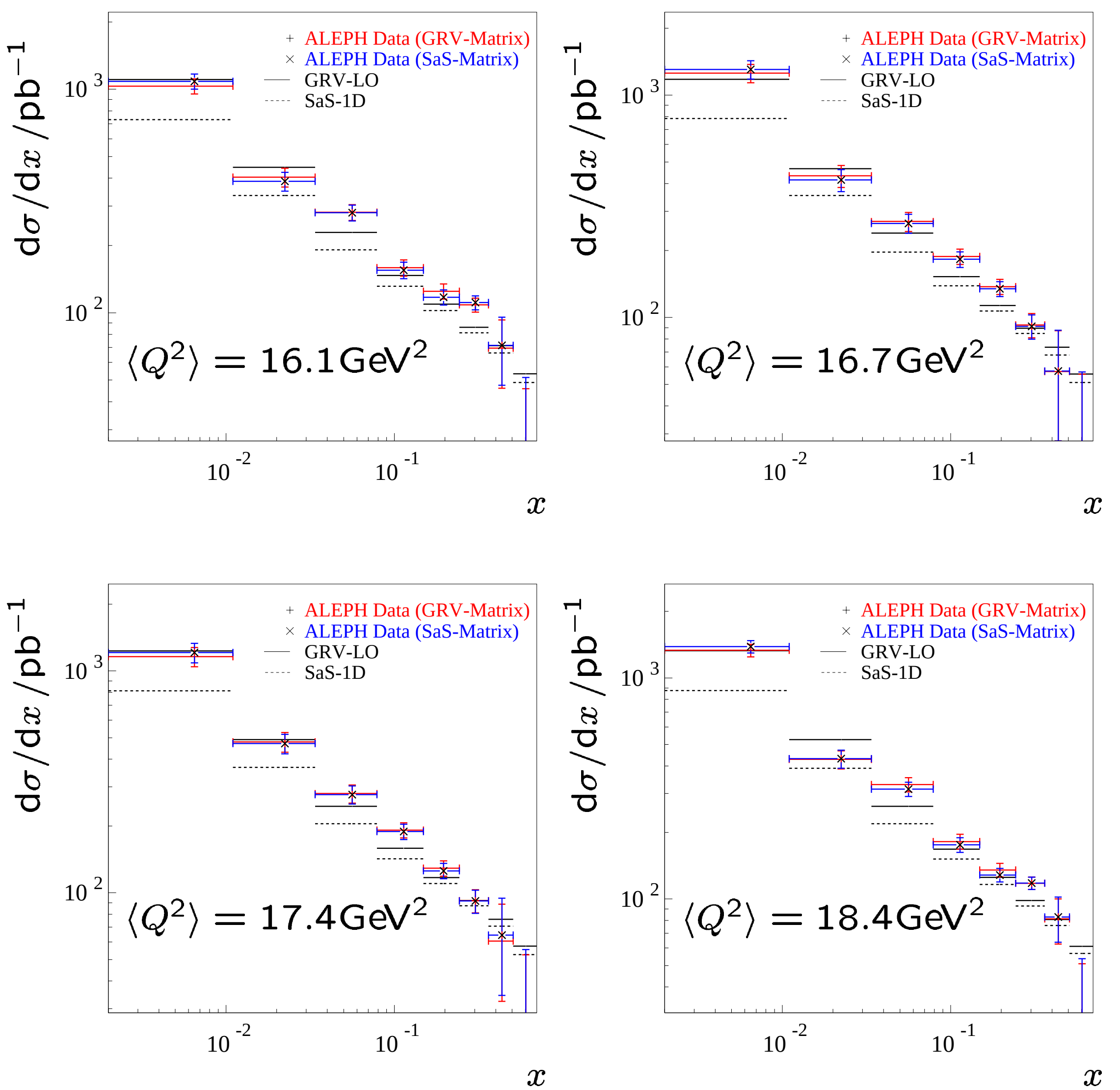

Differential Cross Sections

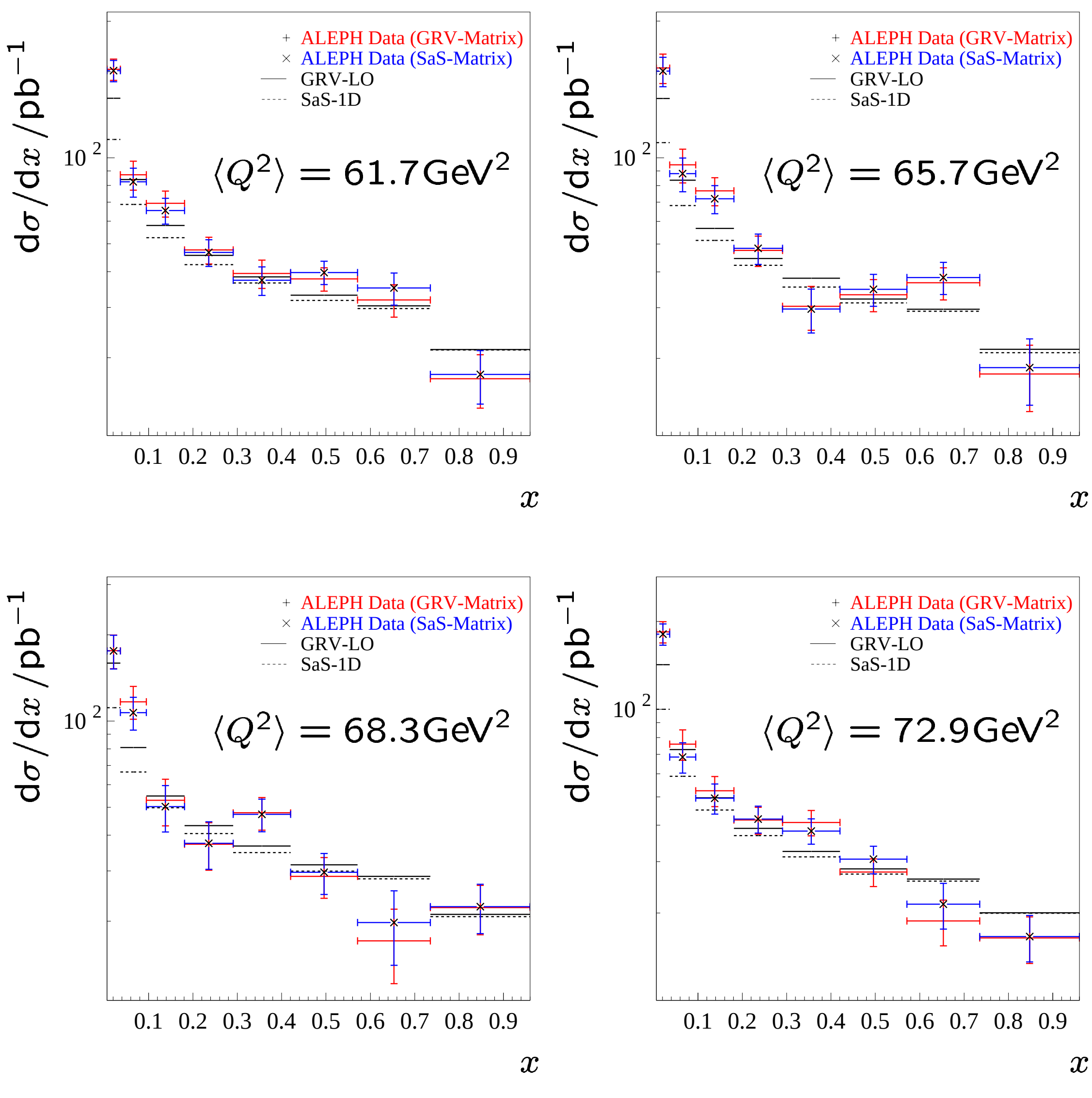

Monte Carlo tests

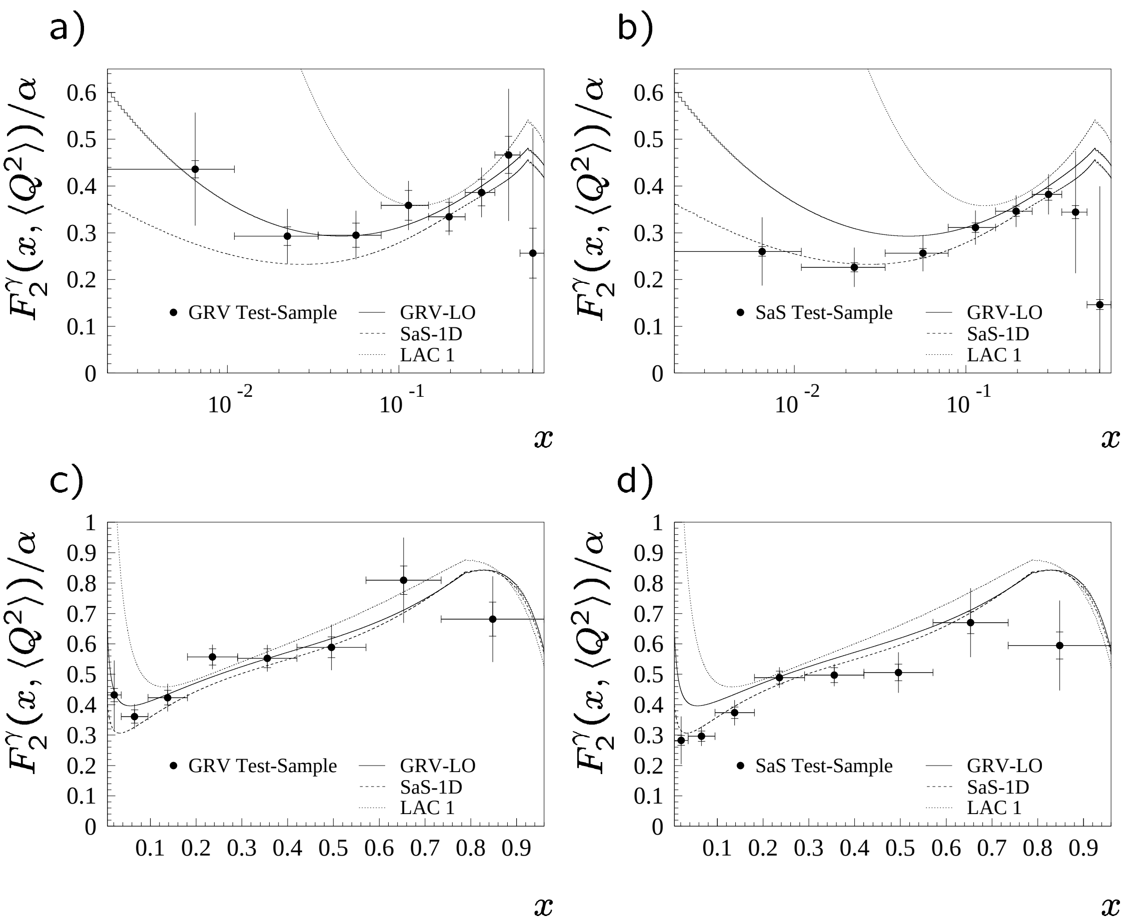

The unfolded structure function $F_2^\gamma(x,\langle Q^2\rangle)/\alpha$ for Monte-Carlo test samples of the same size of the data sample used in this analysis. The test samples are subject to exactly the same analysis procedure as the data. The outer error bars give the total uncertainty, the inner marks show the statistical uncertainty only. The systematics include all contributions except fragmentation.

Results

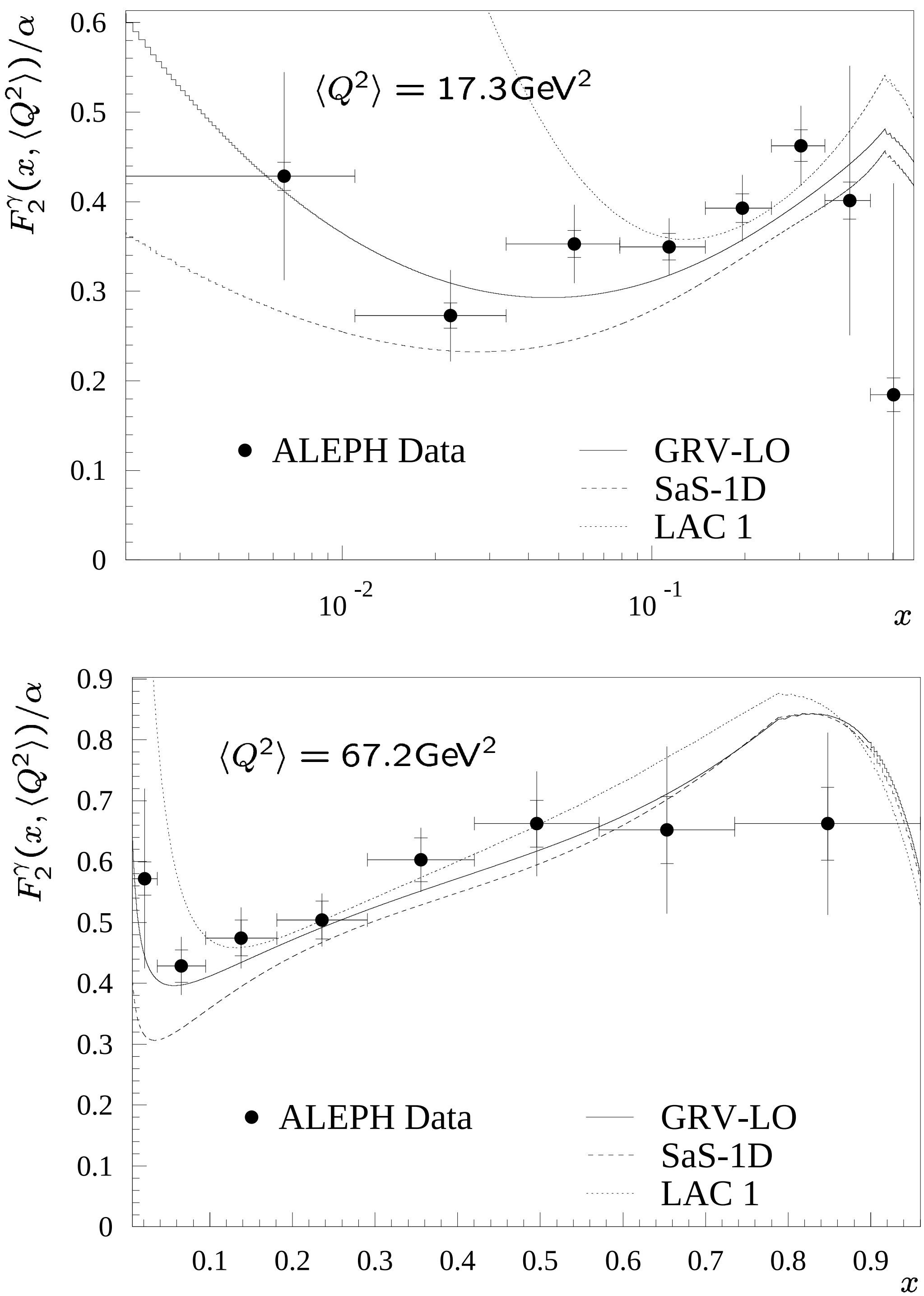

The measured values of F_2^γ/α. The results for all centre-of-mass energies are combined using the luminosity of the data samples as weight. Inner error bars indicate statistical errors only.

Results

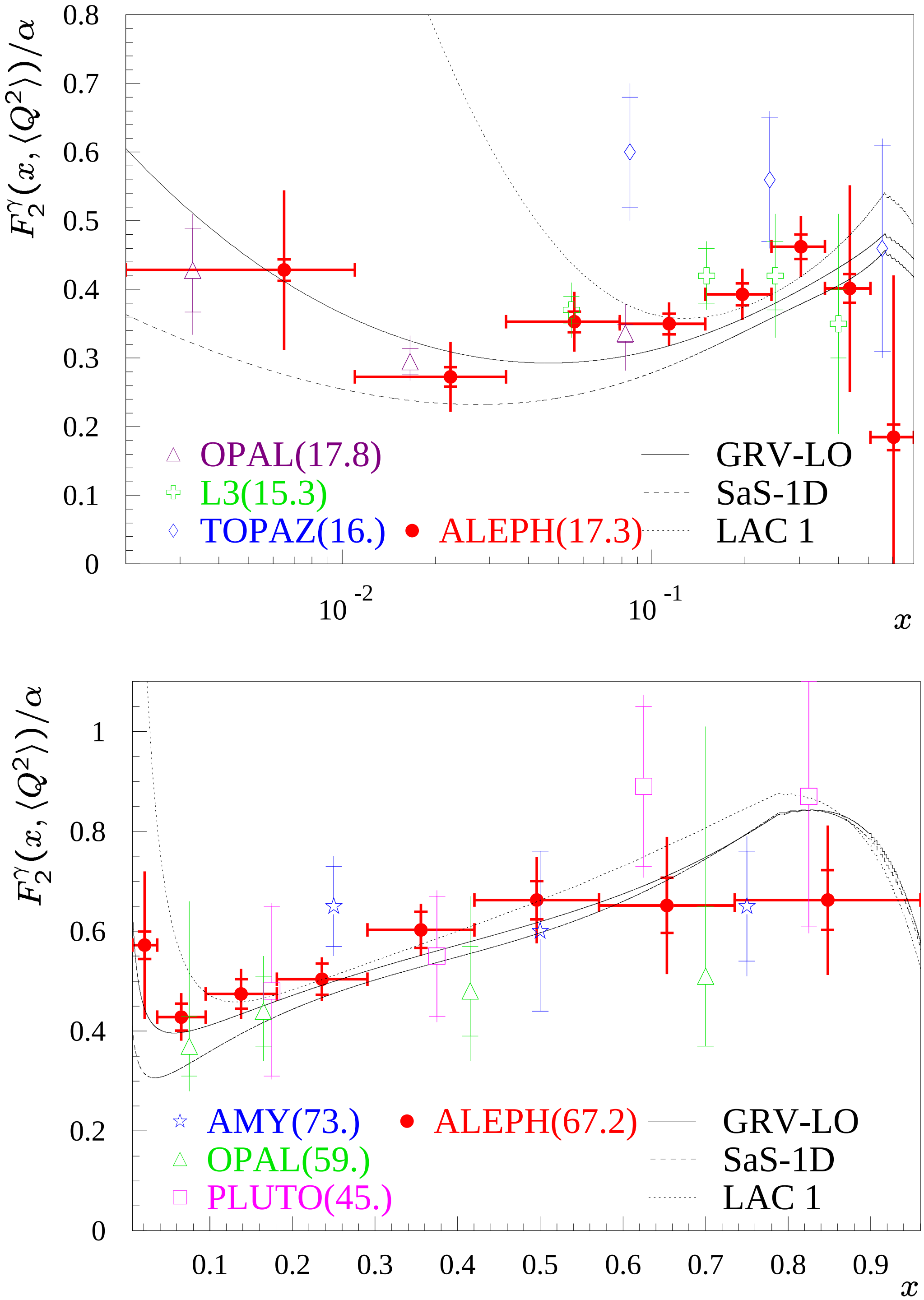

The values of F_2^γ/α from this analysis compared to earlier measurements for similar values of $\langle Q^2 \rangle$. Inner error bars indicate statistical errors only if available from the publications.

Results for low Q^2

$\langle Q^2 \rangle = 17.3\text{GeV}^2$								
x Bin	F_2^γ	Uncertainties						
		Total	Stat.	System.	Approx.	Frag.	Model	others
0.002 - 0.011	0.43	0.116	0.016	0.115	0.017	0.108	0.010	0.035
0.011 - 0.034	0.27	0.051	0.014	0.049	0.006	0.045	0.005	0.018
0.034 - 0.079	0.35	0.044	0.015	0.041	0.008	0.032	0.005	0.024
0.079 - 0.149	0.35	0.032	0.015	0.028	0.007	0.003	0.003	0.027
0.149 - 0.243	0.39	0.037	0.016	0.034	0.003	0.007	0.009	0.032
0.243 - 0.362	0.46	0.045	0.018	0.041	0.024	0.018	0.003	0.027
0.362 - 0.507	0.40	0.150	0.021	0.149	0.136	0.003	0.017	0.058
0.507 - 0.700	0.18	0.236	0.019	0.235	0.227	0.007	0.009	0.060

Measured values of F_2^γ and their uncertainties.

Results for high Q^2

$\langle Q^2 \rangle = 67.2\mathrm{GeV}^2$								
x Bin	F_2^γ	Uncertainties						
		Total	Stat.	System.	Approx.	Frag.	Model	others
0.006 - 0.036	0.57	0.148	0.027	0.145	0.018	0.142	0.005	0.026
0.036 - 0.095	0.43	0.048	0.027	0.039	0.009	0.012	0.017	0.032
0.095 - 0.181	0.47	0.050	0.029	0.041	0.011	0.017	0.014	0.033
0.181 - 0.291	0.50	0.044	0.031	0.031	0.009	0.007	0.003	0.028
0.291 - 0.420	0.60	0.052	0.036	0.038	0.013	0.007	0.010	0.033
0.420 - 0.571	0.66	0.086	0.038	0.077	0.007	0.064	0.014	0.041
0.571 - 0.736	0.65	0.138	0.055	0.126	0.029	0.086	0.041	0.077
0.736 - 0.960	0.66	0.150	0.060	0.137	0.069	0.076	0.022	0.089

Measured values of F_2^γ and their uncertainties.

Correlation Coefficients

$\langle Q^2\rangle = 17.3\text{GeV}^2$								
x Bin	1	2	3	4	5	6	7	8
1	1.00	-0.51	0.07	0.12	-0.08	-0.03	0.03	0.01
2		1.00	-0.50	-0.09	0.27	-0.03	-0.08	0.01
3			1.00	-0.37	-0.46	0.27	0.16	-0.06
4				1.00	-0.02	-0.66	0.01	0.16
5					1.00	0.06	-0.67	-0.01
6						1.00	0.36	-0.50
7							1.00	-0.02
8								1.00

$\langle Q^2\rangle = 67.2\text{GeV}^2$								
x Bin	1	2	3	4	5	6	7	8
1	1.00	-0.48	0.01	0.20	-0.11	-0.02	0.04	-0.02
2		1.00	-0.45	-0.26	0.32	-0.04	-0.07	0.04
3			1.00	-0.23	-0.52	0.34	0.01	-0.05
4				1.00	-0.12	-0.71	0.39	-0.11
5					1.00	0.04	-0.71	0.42
6						1.00	-0.10	-0.30
7							1.00	-0.53
8								1.00

Statistical correlation coefficients for the results of the F_2^γ measurement.

Q^2-Evolution

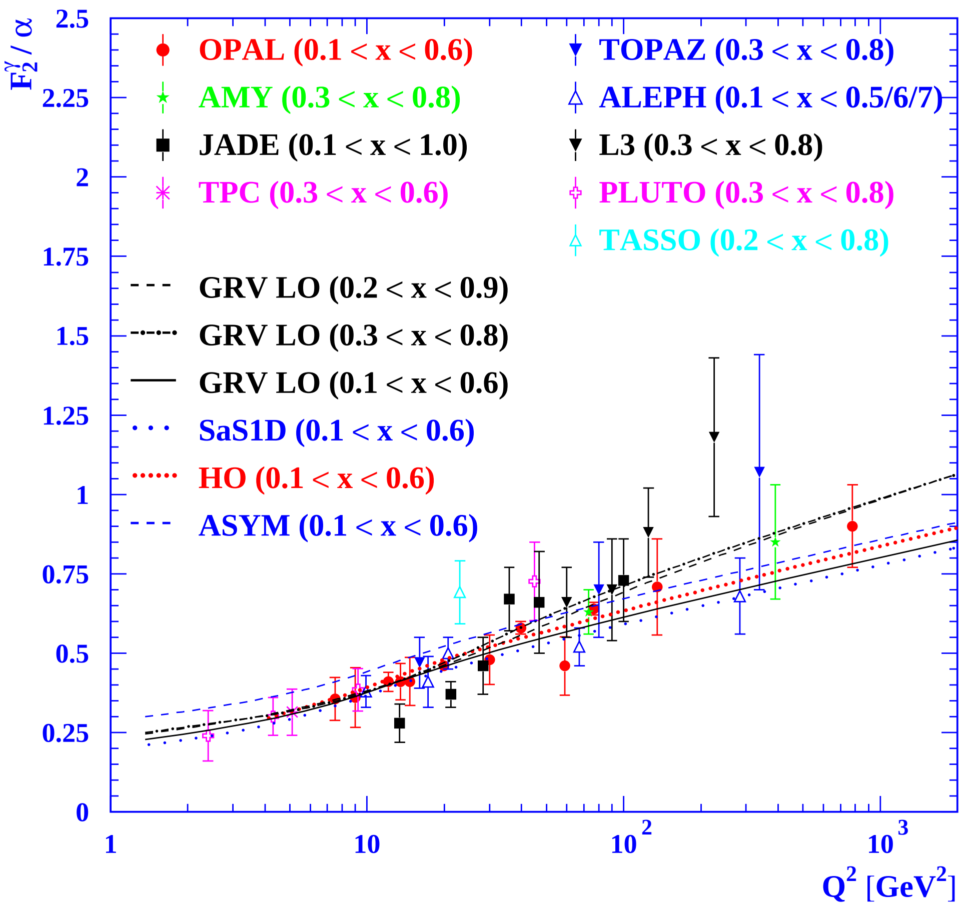

Q^2 evolution for medium values of x measured by different experiments. The result from this analysis is included for

$$\langle Q^2 \rangle = 17.3\text{GeV}^2 \text{ and } 0.1 < x < 0.5$$
and for
$$\langle Q^2 \rangle = 67.2\text{GeV}^2 \text{ and } 0.1 < x < 0.7.$$

Conclusions

- Acceptance and resolution of the detector require a regularized unfolding method.
- A measurement of the hadronic photon structure function $F_2^{\gamma}(x, Q^2)$ could be performed in two different bins in Q^2. A standard Tikhonov unfolding was successfully used.
- Different sources of uncertainties due to regularization and the detector response matrix were discussed.
- The measurement is limited by systematic uncertainties.
- Results agree with common theoretical predictions.